

pubs.acs.org/acsapm Article

Electrospun Thermosetting Carbon Nanotube-Epoxy Nanofibers

Nojan Aliahmad, Pias Kumar Biswas, Vidya Wable, Iran Hernandez, Amanda Siegel, Hamid Dalir,* and Mangilal Agarwal*



Cite This: ACS Appl. Polym. Mater. 2021, 3, 610-619

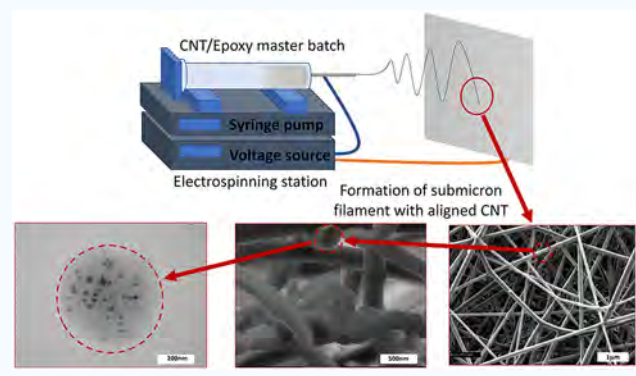


ACCESS

III Metrics & More

Article Recommendations

ABSTRACT: This paper represents the process of fabrication and characterization of submicron carbon nanotube (CNT)—epoxy nanocomposite filaments through an electrospinning process. Electrospinning is one of the most versatile, inexpensive, and environmentally well-known techniques for producing continuous fibers from submicron diameter all the way to tens of nanometer diameter. Here, electrospinning of submicron epoxy filaments was made possible by partial curing of the epoxy by mixing the hardener and through a thermal treatment process without the need for adding any plasticizers or thermoplastic binders. This semicuring approach makes the epoxy solution viscous enough for the electrospinning process, that is, without any solidification or nonuniformity caused by the presence of the hardener inside the mixture. The filaments were spun using a CNT/epoxy solution with



a viscosity of 65 p using 16 kV and a collector distance of 10 cm. The diameter of these filaments can be tuned as low as 100 nm with adjustment of electrospinning parameters. By incorporating a low amount of CNT into epoxy, better structural, electrical, and thermal stabilities were achieved. The CNT fibers have been aligned inside the epoxy filaments because of the presence of the electrostatic field during the electrospinning process. The modulus of the epoxy and CNT/epoxy filaments were found to be 3.24 and 4.84 GPa, respectively. The presence of the CNT can lead up to 49% improvement on modulus. Accordingly, using a commercially available epoxy suitable for industrial composite productions makes the developed filament suitable for many applications.

KEYWORDS: epoxy, CNT, filaments, nanocomposites, thermosetting

INTRODUCTION

With the emergence of nanotechnology, researchers all over the world have been extensively devoting efforts to the preparation and discovery of new nanocomposites for various commercial applications. 1-4 The advantage of making these nanocomposites is to achieve better properties such as higher mechanical properties, thermal stability, and efficiency. Nanocomposites can be formed in different shapes such as flakes, fibers, and hybrids.5 Several research studies have been conducted to extrude nanofilaments made out of neat thermoplastic epoxy and nanocomposites.⁶ Despite the research and progress on making composite-based nanosized filaments, the fabrication of a thermosetting nanocomposite has still remained a challenge. There are several limiting factors of making a continuous filament out of thermosetting epoxy, while the thermosetting polymers are limited to be extruded or stretched. Furthermore, having a uniform nanocomposite by adding nanomaterials to the thermosetting epoxy composite is still a challenge. In this paper, an electrospinning-based approach has been developed and tested to overcome the

limits of fabricating a nanocomposite thermosetting epoxy filament with diameters in the nanoscale range.

Compared to contemporary approaches for fabricating continuous nanofibers, electrospinning, which involves electrohydrodynamic phenomena, is widely acknowledged as the most versatile, effective, and economically beneficial process. This simple voltage-driven, electrostatic method only requires a pump, a high voltage power source, a collector, and a solution reservoir tipped with a blunt needle. Voltage, flow rate, needle-collector distance, viscosity, and the type of solvents all represent key parameters in regulating the properties of the fibers created through electrospinning. Different polymers have been examined in the past and have

Received: May 18, 2020 Accepted: November 19, 2020 Published: December 28, 2020





been shown to be compatible with electrospinning. 13 The uniform polymer nanofiber structures formed by electrospinning have been reported to have diameters ranging from 2 nm to several microns¹³ and exhibit superior properties such as high surface area to volume ratio, flexibility in surface functionalities, 14 inter/intra fibrous porosity, and extraordinary mechanical properties.

Thermosetting epoxy nanofibers are gaining tremendous popularity in many structural applications such as interlayer reinforcement in carbon fiber reinforced polymer (CFRP) composites. However, the production of these fibers at the nanoscale has never been achieved. Nanofibers synthesized via electrospinning of thermoplastic polymers such as polyaniline (PANI), polyvinylpyrrolidone (PVP), polyvinyl alcohol (PVA), polycaprolactone (PCL), and so forth¹⁵ have been investigated in the development of thermoset-thermoplastic blending and core sheath to fabricate such fibers (e.g., polycaprolactone/epoxy^{16,17} and polyacrylonitrile/epoxy¹ However, the presence of thermoplastic content in the resulting fibers can deteriorate their mechanical properties, especially under elevated thermal conditions. The removal of the sacrificial thermoplastic polymer after electrospinning, in a way that does not adversely influence the properties of the resin, has represented a nearly impossible challenge. However, the innovative proposed approach is specifically developed to increase the spinnability of a widely used commercial thermosetting polymer to produce nanofibers that do not require destructive postprocessing.

The overarching goal of this work is to create fibers that could be electrospun along with nanoreinforcements such as carbon nanotubes (CNTs) to produce nanohybrid fibril nanocomposites with an enormous surface area and surface compatibility to be used with epoxy matrices in advanced diversified composite applications. ¹⁹⁻²³ The degree of dispersion of the nanoparticles into the polymer matrix always influences the electromechanical characteristics of the final products. Accordingly, the CNT is one of the best candidates to make nanocomposites, because of its extraordinary mechanical properties. 26-29 Although CNT-based nanocomposites have been developed for many consumer and industrial products (such as Babolat tennis racquets and Baltic Yacht),³⁰⁻³² major limitations prevent large-scale industrial manufacturing. Most of these nanocomposites are made by an extensive amount of CNT (not a cost-effective approach³³). In addition, the lack of good CNT dispersion shows an unexpectedly large increase in the viscosity of epoxy resins.³⁴ Industry-graded thermosetting epoxy nanocomposites with mechanically dispersed multiwalled CNTs have been studied

Because of the need for making CNT/epoxy-based nanocomposites, different research studies have been conducted to make a uniform composite structure. The low dispersion of the CNT inside the epoxy structure results in the formation of clusters because of the van der Waals forces.³⁷ The lack of uniform dispersion of the CNT inside the epoxy results in the reduction of mechanical properties of the composite. Recently, there have been multiple research studies on making uniform CNT/epoxy structures. As it was reported by Roy et al., using functionalized CNTs can improve the uniformity of the nanocomposite. Carboxylation of the CNT improves the surface potential of the nanofiber and makes it more soluble in epoxy solvents.³⁸ Functionalization might reduce the properties of the CNT, so using physical mixing is more desired to

make CNT/epoxy structures.³⁹ Multiple methods have been used to develop a well-mixed CNT/epoxy solution such as high-speed steering, mechanical mixing, roller mixers, ultrasonic radiation, and a mixture of these methods. As it was reported by Barra et al., applying mechanical and ultrasound mixing is the best method of making uniform separation of the CNT inside an epoxy structure.³⁷ In using this combined method, the CNT will be separated uniformly inside the structure by mechanical steering, while sonication helps the separation of clusters. The byproduct of this sonication is large amount of heat which is not suitable for the epoxy hardener solution. Although the presence of heat solidifies the epoxy/ hardener mixture, perfect timing and combination are needed to mix the CNT in epoxy hardener solutions. Still, to date, controlled dispersion of CNTs for electrospinning has remained a challenge mostly for a thermosetting polymer matrix such as epoxy. This is due to the Van der Waals binding energies related to the CNT aggregates, creating clusters and nonuniform networks inside the polymer. Thus, a method is needed to separate the fibers to prevent clustering and make the uniform formation of the CNT inside the structure. As it was previously reported, the CNT polymer matrix has been developed using thermoplastic polymers through an electrospinning process to achieve unidirectional CNT structures, while not adversely impacting the weight of the composite.⁴⁰ Despite multiple research studies on the fabrication of CNT composite nanofibers using thermoplastic polymers through an electrospinning process, there has been no significant research on using thermosetting polymers. 40-42 Because of high viscosity of thermosetting polymers, adding any nanomaterials such as CNTs can generate clusters in the structure, reducing the uniformity and making it less suitable for electrospinning. In this paper, we present a uniform dispersion of the CNT in the epoxy polymer that utilizes a multistep mixing strategy. Here, based on forced extrusion of the CNT-epoxy nanocomposite followed by electrospinning, unidirectional alignment of CNTs within electrospun epoxy nanofibers was achieved.

Solution parameters (e.g., polymer concentration, viscosity, conductivity, and surface tension), process parameters (e.g., applied voltage, distance between the capillary tip and collector, and flow rate of the polymer solution), and ambient parameters (temperature and humidity)^{43–46} have been carefully considered to optimize the sensitized nanofiber morphology. This work shows how to obtain CNT-based epoxy nanofibers to achieve greater mechanical characteristics in a simple and cost-effective way from an industrial perspective. Our method for CNT dispersion and nanofiber formation via electrospinning is easily scalable to higher manufacturing readiness levels.

MATERIALS AND METHODS

A masterbatch of nonfunctionalized CNTs was used as nanoreinforcements to be mixed with epoxy. The masterbatch consists of epoxy resin based on bisphenol A (50-99 pbw %), ethanol solvent (<15% volume), and CNTs (5 wt %). The diameter of the nanotubes is in the range of 5-50 nm, with lengths in the 2-3 μ m range. The nanoreinforcement via masterbatch was chosen to avoid CNT suspension and to facilitate the dispersion process. Additionally, dimethylformamide (DMF) and Triton X-100 were also effective at separating and suspending CNTs. Epikure 3234 (triethylenetetramine, Miller-Stephenson, USA) was used as the curing agent and was supplied by Hexion specialty chemicals. Samples were prepared by mixing masterbatch and DMF (1:4 volume ratio) for 10 min using a

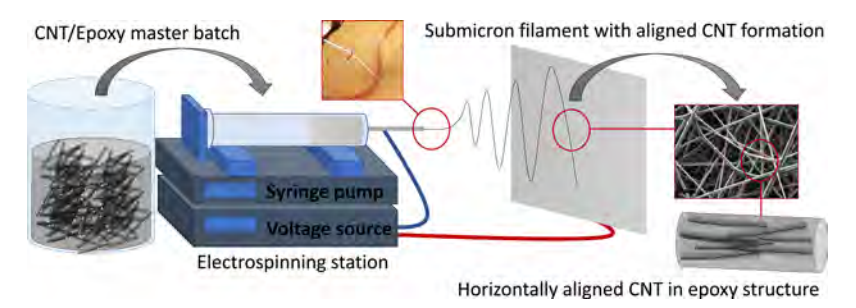


Figure 1. Process schematic for making a submicron CNT/epoxy filament through electrospinning.

magnetic stirrer (600 rpm), followed by probe sonication for 10 min in intervals of 45 and 30 s rest between cycles (200 W, 20% amplitude, 8-2 s pulse). To achieve lower concentration of CNTs (2 and 4 wt %), the master batch was mixed with more epoxy. Triton X-100 was then added into the mixture in the ratio of 20:1 and was stirred for 10 min, followed by sonication in the same manner as before. Neat epoxy was added in the same weight as masterbatch and stirred for 15 min, followed by the same sonication method. The curing agent was then added to the mixture at a ratio of 15:1 and was allowed to stir at 50 °C for 2 h in order to obtain a homogeneous solution. The mixture was degassed in a vacuum oven at room temperature for a minimum of 15 min and was then allowed to rest for at least 24 h before electrospinning. Prior to spinning, the prepared solution was added to a syringe with a needle gauge of 26 G. The pumping rate of the epoxy solution was adjusted to 0.5 mL/h. An electrospinning voltage of 16 kV was applied between the needle and collector at room temperature and a needle tip/collector distance of 10 cm. The collector plate for this experiment was a 20 cm by 20 cm rectangular platinum plate. At a critical voltage (between 12 and 16 kV), a jet of a solution emerged from the needle tip and was accumulated on the collector for 10 min and stored in a vacuum oven at room temperature for 10 min. The process of making submicron CNT/epoxy filaments is shown in Figure 1. All the chemicals used in the experiments have been provided by Sigma-Aldrich, USA, unless it is noted.

The quality of the fabricated composite was checked using a 785 nm Foster and Freeman microlaser Raman. Fiber formation and size were analyzed by field emission scanning electron microscopy (FESEM; JEOL 7800F, JEOL Japan). Modulus of the fibers was measured using atomic force microscopy (Bruker, USA). X-ray photoelectron spectroscopy (XPS) and thermal gravimetric analysis (TGA) were conducted with an Omicron XPS/UPS system with an Argus detector (ScientaOmicron, Germany) and a TA instruments SDT Q600 TG thermal analyzer (TA, USA). The mechanical properties have been measured using a Bruker Catalyst atomic force microscope mounted on a Leica DMI3000 inverted optical microscope (Bruker, USA) and Test Resources 100 series (Test Resources, USA) according to the ASTM D3039 standard.

■ RESULTS AND DISCUSSION

CNT/Epoxy Composite. Morphology and uniformity of the fabricated epoxy composite have been analyzed. The CNT/epoxy batch was observed after preparation and showed no phase separation after 24 h, and the solution was still dark black after adding the CNT. Further formation of the CNT within the epoxy structure after curing was investigated using Raman spectroscopy and SEM. A comparison between the Raman spectra of the epoxy alone and the CNT/epoxy is shown in Figure 2. Raman spectroscopy results revealed that by adding the CNT, the peaks for D bands 1315–1310 cm⁻¹ have been increased, which is related primarily to sp³ bonds of CNTs, and the G band from 1607 to 1620 cm⁻¹ remains almost constant, which is related to in-plane sheet sp²-hybridized carbon. Here, the presence of the D band proves

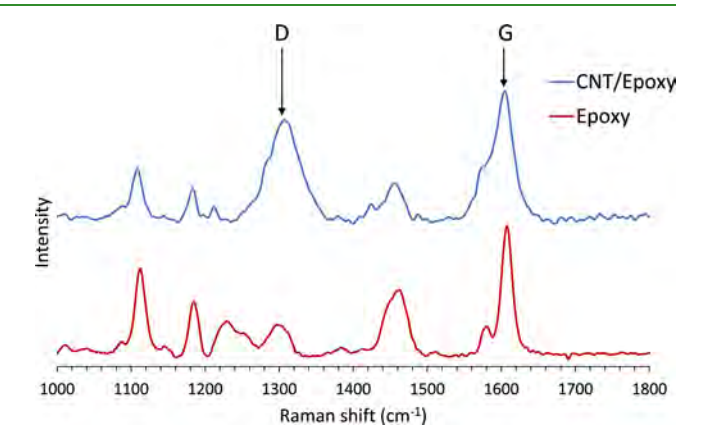


Figure 2. Raman spectra of cured CNT/epoxy and epoxy samples, and the D and G bands are marked to reveal the presence of the CNT in the structure of the composite.

the formation of the CNT inside the epoxy structure. Although epoxy is also carbon-based, the G band is related to the sp² hybridization of carbon in this material. Adding the CNT to the structure improves the D band and shows a change in uniformity of the CNT inside the epoxy structure.

SEM analysis revealed that the CNT is uniformly mixed within the epoxy solution. In addition, no significant change in the morphology of the epoxy was observed. This uniform distribution retains the properties of epoxy, while improving its mechanical and electrical properties. The uniform formation of the CNT is due to the presence of DMF, as a polar solvent, and adding plasticizers to prevent clustering. Figure 3a shows the SEM image of the resulting CNT/epoxy sample, where CNT rods were found in the cross-sectional view of the cured CNT-epoxy masterbatch sample. CNT-epoxy fibers showed the uniform formation of the randomly sorted CNT inside the epoxy structure, Figure 3b. A higher magnification image, Figure 3c, of the same structure showed uniformity of the CNT network inside the CNT/epoxy composite. Electrospinning of 2 and 4 wt % CNT-epoxy composites here helped to form unidirectional randomly sorted CNT rods inside the core of epoxy fibers. It was also realized that by increasing the amount of CNT, at first, the mixture kept its integrity and uniform structure, but by increasing the weight of the CNT to 8 wt %, clusters of the CNT started to form in the mix. This phenomenon makes the solution made by a higher CNT concentration in epoxy less suitable for electrospinning. Because of this observation, all the samples for this manuscript have been made by 2 and 4% weight of the CNT.

CNT/Epoxy Submicron Filaments. Filament Fabrication. Rapid change in thermoset resin viscosity makes the fabrication of an electrospun filament challenging, while there

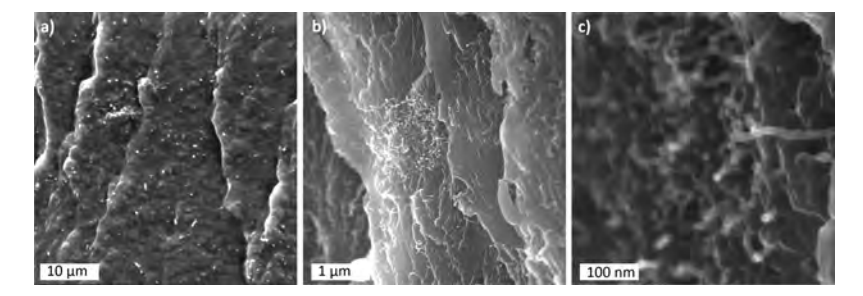


Figure 3. SEM images of the cryofracture CNT/epoxy sample revealing (a) CNTs inside the CNT-epoxy structure before electrospinning, (b) the formation of CNTs inside the CNT-epoxy structure, and (c) uniformity of the CNT network inside the CNT/epoxy composite using higher magnification.

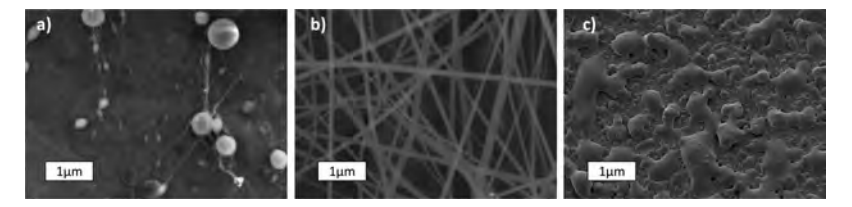


Figure 4. SEM images of electrospun CNT/epoxy solutions after (a) 5, (b) 20, and (c) 30 h resting time.

is no added thermoplastic to the solution. To achieve a spinnable viscosity, the epoxy mixture was adjusted using a partial curing method. The partial curing of the thermosetting epoxy helped to achieve enough viscosity to make it spinnable, but not completely cured. Electrospinning is based on the extraction of polyelectrolytes in the form of ionized polymers; thus, the Epon epoxy, which is based on bisphenol F, can be ionized and used for electrospinning. The main issue is adding the hardener, which causes instant solidification and makes the epoxy not suitable for electrospinning. Otherwise, removing the hardener also causes structural failure for spun fibers. The epoxy with no hardener is not viscous enough because of the lack of polymer chain formation, so it is not spinnable. In this method, adding the CNT and partially curing the epoxy/ hardener is the key to make submicron fibers through electrospinning. By adding highly conductive CNT nanofibers in the epoxy structure, the ionization of the solution will

To check the partial curing process, samples were made with different resting times (5, 20, and 30 h) and the quality of the resulting fibers was investigated using SEM. Figure 4 shows the change in fiber formation as a result of the partial curing resting time. It was found that the lowest resting time (5 h) was not enough to ensure proper chemical bonding between the epoxy and hardener. Thus, the viscosity is still in the range of 5 p. In contrast, higher rest time (30 h and more) almost fully cured the epoxy and resulted in high viscosities in the range of 500 p, preventing the solution to be spinnable. At lower viscosity (i.e., shorter rest time), the filament cannot form because during the electrospinning process, the surface tension of the solution and high electric field produce fragments by entangling the polymer chains. At higher viscosity (i.e., longer rest times), the mixture overcomes the surface tension of the solution, and consequently, uniform fibers can be produced. By curing the epoxy solution for too long, higher ratios of entangles affect the uniformity of the fibers and lead to the production of large bids. Moreover, further increasing the curing time results in the solid components (fully cured) that completely damage the uniformity of the filament by hampering the solution flow rate through the needle tip and

causing blockages. In this case, the 20 h of resting time is optimum, while the viscosity of the solution reached 65 p, which makes it suitable for electrospinning.

Optimization of the flow rate is also critical as higher flow rates can cause nonevaporation of the solvent and low stretching of the solution in the jet extruded between the collector and needle tip. These conditions ultimately increase the diameter of the nanofibers and the production of beads and ribbon-like structures. In contrast, low flow rates under the critical point can cause failure in the formation of continuous nanofibers, affecting morphology. Here, the flow rates of 0.1–1 mL/h have been investigated. According to the viscosity of the solution, the 0.5 mL/h flow rate made the best possible fibers. In higher pumping ratios (above 0.7 mL/h), electrospraying starts, so instead of having filaments, the uniform layer of CNT/epoxy is achieved, while in lower flow rates (less than 0.4 mL/h), filaments are not extruding according to the lack of epoxy solution supply.

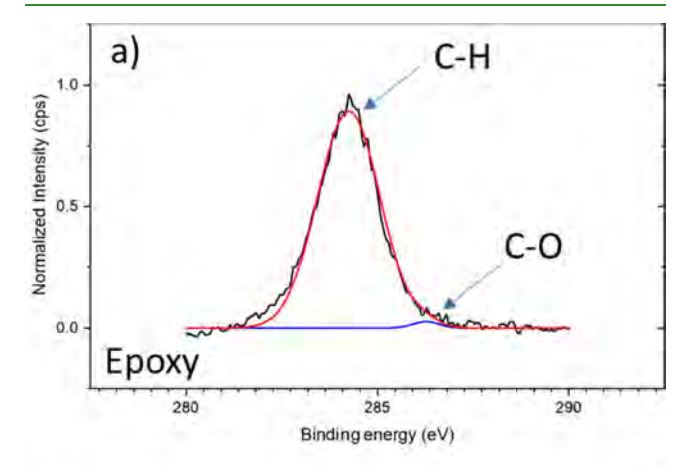
The distance between the needle and the metallic collector also plays a vital role. Several parameters must be optimized considering the deposition time of the polymer solution, the evaporation rate of the solvent, and whipping or instability interval. 12,47 If the distance is kept relatively small, the potential for beaded and large-diameter nanofibers is increased.⁴⁸ In this case, 10 cm distance is the optimum. Polymeric concentration with increased viscosity increases the chain entanglement among polymer chains and smooths the formation of continuous nanofibers. However, extreme viscosity can completely block the needle tip or start the formation of scattered beaded nanofibers with nonuniform diameters.⁴⁹ Figure 4 shows the SEM images of the different electrospun samples that were cured at different times. As is shown here, 20 h was the best resting time to make submicron filaments. Table 1 shows the settings which were used for each submicron fiber made of specific CNT concentration.

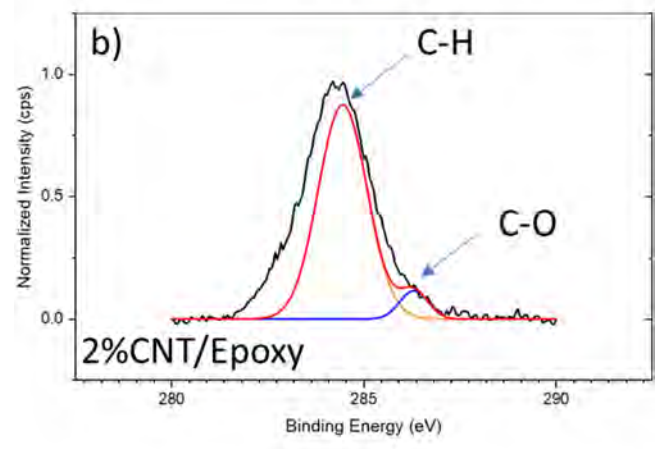
Surface element compositions of neat epoxy, 2 and 4% wt. CNT/epoxy composite electrospun fibers were analyzed by XPS spectra. Every peak is fitted using standard carbon binding energy where the principal peaks of neat epoxy and modified epoxy have almost similar binding energy. For example, the

Table 1. Electrospinning Setting Parameters for Different CNT/Epoxy Concentrations

CNT percentage (%)	cured time (h)	viscosity (p)	voltage (kV)	flow rate (mL/h)	distance between needle and collector (cm)
0	20	65	16	0.5	8-10
2	16	65	16	0.4	9-10
4	15	68	16	0.4	10-10.5

signature of the hydrocarbon peak $(-C_xH_y-)$ has been identified for all epoxy types (Figure 5a-c) at a binding





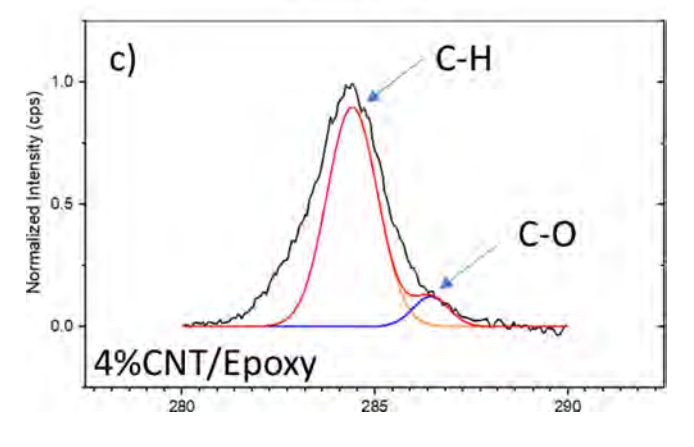


Figure 5. X-ray photoelectron spectroscopy spectra of the epoxy composite (a) with no, (b) with 2%, and (c) with 4% CNT; the results show the formation of a higher number of C–O bonds by increasing the CNT concentration and improving the crystalline structure of the composite.

energy of 284.6 eV which is attributed to sp²-hybridized graphite-like carbon atoms and sp² carbon atoms bound to hydrogen. However, Gaussian peaks for 2 and 4% wt CNT/ epoxy are observed differently. A sharp peak of carbon atoms bound to oxygen atoms by a single bond such as alkoxy groups (C-O) starts to form with a binding energy of 286.2 eV⁵⁰⁻³ for both (Figure 5b,c), which is originated from sp³-hybridized carbon atoms and is similar to that of the diamond-like carbon. A minor peak at 287.3 eV is observed as well, which is assumed to be carbon atoms bounds with oxygen by a double bond (C=O). Here, the analysis also demonstrates that by adding the CNT, the formation of alkoxy groups becomes more dominant, and this can result in having stronger bonding between polymer chains inside the structure. The results indicate that adding more CNTs renders in a higher count of the C-O/C=O bonding and formation of a more chemically and mechanically stable polymer. 51,53

Figure 6 shows the cross section and top-view SEM image of fabricated submicron fibers. As it is noted in Figure 6a, the deposited nanocomposite structure provides a highly porous layer. The thickness of this layer is adjustable by setting spinning parameters and the time of electrospinning. The actual size of the fibers was found to be in the range of 100-500 nm along with a uniform distribution. Furthermore, a high magnification cross section revealed that the CNT nanofibers were unidirectionally embedded inside the epoxy structure. This formation is well suited for many applications spanning sensors, reinforcements, and different membranes. 54,55 This formation is due to the applied electric field throughout the electrospinning process. The high electric field moves the direction of the highly conductive CNT rods, while the epoxy solution is still not fully cured. Later, by extrusion of the filament, the outer shell of the filament begins to dry and retains the CNT formation in one direction. Another identification from SEM images is that by increasing the amount of CNT in the epoxy mixture, the fibers become thinner, resulting in much stiffer fibers. Figure 6b-d shows the top view of neat epoxy, 2 wt % CNT/epoxy, and 4 wt % CNT/ epoxy, respectively. The identification of the images reveals that the fibers become thinner by increasing the amount of CNT. The stronger fibers can be stretched more and make thinner filaments through the electrospinning process. The histogram of each batch has also been provided in Figure 6e to compare the size and uniformity of the fibers. As it is shown here, the 4% has the smallest average diameter in the range of 250 nm, while the 2% average is close to 350 nm and 0% is around. The distributions of the thicknesses are based on the same pattern, showing the uniform formation of fibers and adjustability of the method.

Uniformity of the developed fibers was also observed using STEM and TEM. Figure 7a shows a STEM image of the side view of a filament and (b) reveals the cross section of a filament. STEM highlights the size of the fibers and the formation of a unidirectional CNT network inside the epoxy structure. Later, the side view STEM of the fibers revealed that although CNT rods are made, some clusters and some of these rods are bent, but the majority of the clusters and fibers are semialigned in the direction of the electric field. As noted in Figure 7, the formation of CNT rods inside the filament has been investigated, and subsequently, TEM imaging also proved the formation of the CNT network. Figure 7c,d shows a TEM image of a filament cross section and side. Here, the formation of CNT rods toward the direction of the filament has been

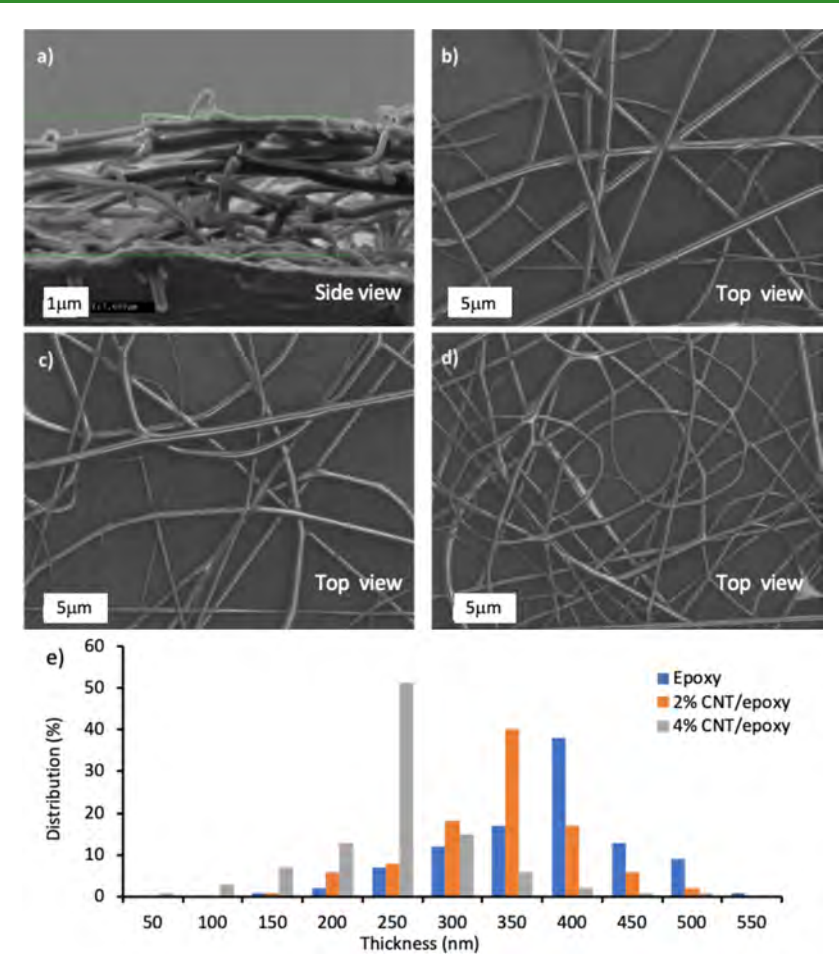


Figure 6. Submicron filament scaffold (a) side view and top view, (b) neat epoxy, (c) 2 wt % CNT/epoxy, and (d) 4 wt % CNT/epoxy; the uniform formation of the CNT inside the epoxy structure using electrospinning has been shown in the cross-sectional image; (e) histogram of fiber size with different CNT concentrations.

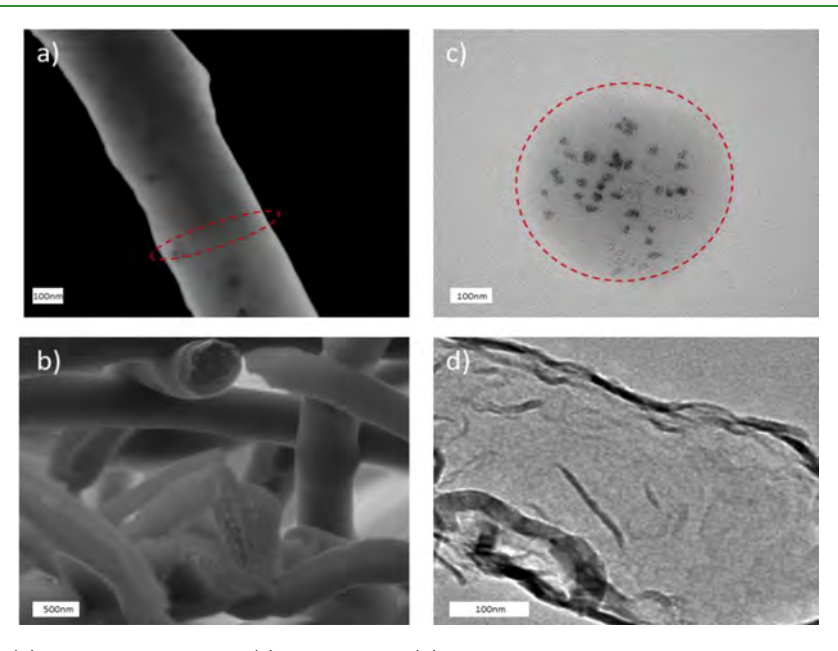


Figure 7. (a) Top-view and (b) side-view STEM, and (c) top-view and (d) side-view TEM images of the electrospun CNT/epoxy fiber, revealing the thickness range, uniformity, and unidirectional formation of CNT clusters within the polymer structure.

revealed. It is also observed that this formation is unidirectional because of the presence of an electric field and the electrical conductivity of the CNT network. This network exists; while the length of the CNT is larger than the diameter of the filament, the CNT rods in the presence of an electric field must be aligned toward the length of the filaments.

Thermal and Mechanical Analysis of CNT/Epoxy Filaments. TGA is one of the most widely used methods for investigating polymer decomposition at different temperatures and thermal stabilities of materials in general. As it is shown in Figure 8, the thermal stability of the pristine epoxy and 2 and 4

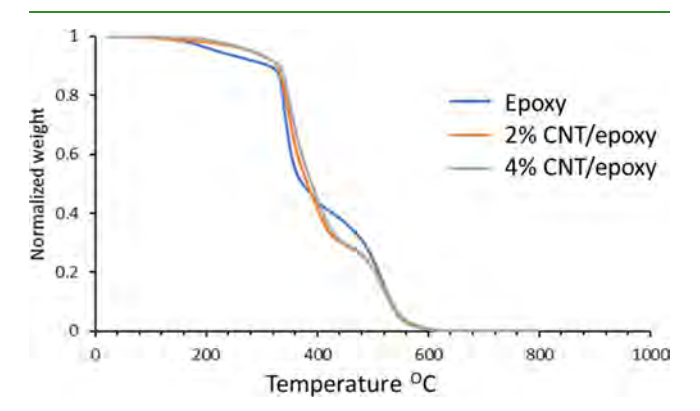


Figure 8. Thermal analysis (TGA) of the CNT/epoxy filament using different CNT concentrations; the thermal analysis reveals the stability of the fibers by adding CNTs.

wt % CNT/epoxy filaments was measured at a heating rate of 10 °C/min in the presence of nitrogen gas. The TGA profile of all these samples showed four steps of degradation behavior. At first, the neat epoxy experienced initial degradation (around 10% weight loss) at $T_{\rm d} \approx$ 360 °C, whereas 2 and 4 wt % CNT/ epoxy composites had similar weight loss at \approx 362 and 365 °C, respectively. This small amount of weight loss is attributed to the desorption of physically absorbed water molecules in the composites.⁵⁶ Then, in the second step where degradation is the maximum (40% weight), neat epoxy degrades faster than the other two counterparts as scanning temperature reached 400 °C. Possibly because CNTs are involved in the lower cross-linking degree, the decomposition rate of 2 and 4 wt % CNT/epoxy composites was slower compared to that of the neat epoxy one.⁵⁷ Interestingly, when the temperature increased to 520 °C, neat epoxy exhibited relatively slow weight decreasing tendency (20% weight). In the last step (temperature range 520-610 °C), all the materials showed similar thermal behavior and decomposed their rest 30% weight at the same rate. Observing all these curves and their

degradation rate at different temperatures, it has been found that the incorporation of CNTs into the epoxy structure has effectively increased the thermal stability of the epoxy composite structure in a small scale.

The surface area and mesopore structure of the electrospun epoxy and electrospun CNT/epoxy were characterized by Brunauer-Emmett-Teller (BET) and N2 adsorption isotherms using an adsorption instrument (Autosorb iQ2), respectively. The nitrogen-adsorption and -desorption isotherms and the pore size distribution of the as-prepared epoxy with 2 wt% nanocarbon content exhibited type V characteristics as Brunauer has defined, which is the most common method used to describe the specific surface area, 58,59 which is indicative of the presence of mesopores in the composites. The measured surface area of the neat epoxy was found to be 219 m²/g compared to a higher area of 304 m²/g for the 2 wt % CNT/epoxy nanofiber. It was confirmed by SEM analysis that adding CNTs will increase the surface area by reducing the fiber diameter. The Barret-Joyner-Halenda (BJH) analyses reveal that for a 2 wt % CNT/epoxy, porosity is in the range of 5-100 nm. This higher surface area makes the developed filaments suitable for interfacial bonding layers.

Figure 9 reveals the improvement of the modulus of the fabricated fibers with the increase in CNT content measured using atomic force microscopy (Bruker Catalyst Atomic Force Microscope). The test was carried out based on the cantilever deflection method. The transverse compression load deformation of the filaments was measured by a rectangular MDNISP-HS (Bruker, USA) tip with a length of 350 μ m and a maximum spring constant of 600 N/m and then used to calculate the modulus of the filament. As it is shown here, by adding more CNTs to the fibers, the mechanical properties have been improved. The modulus has been increased linearly by increasing the CNT content. The measured modulus for neat epoxy is 3.24 GPa, which is in the range of the reported value form the manufacturer, while adding 2 and 4% of CNTs has increased this value up to 4.2 and 4.84 GPa, respectively. Here, the presence of CNTs can lead up to 49% improvement on modulus. As it is shown here, the observed values are in confinement with the rule of the mixture, validating the measured results. To validate the measured results, the rule of the mixture based on the volume concentration and modulus for both CNTs and epoxy has been used to predict the

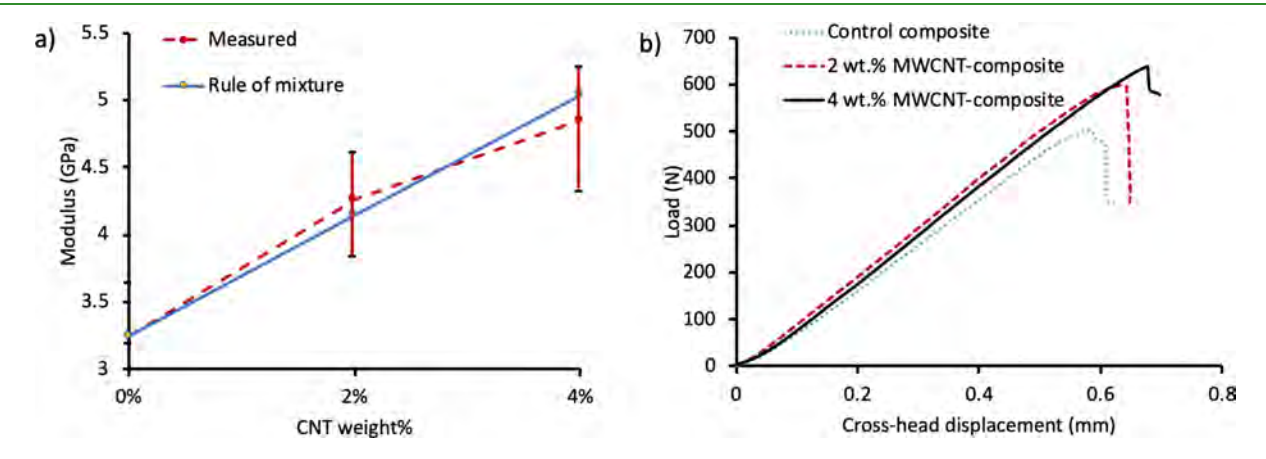


Figure 9. (a) Modulus and weight fraction relation of the CNT/epoxy nanofiber with different CNT concentrations; the observed values are in confinement with the rule of the mixture, validating the measured results; (b) load—displacement curves of the panels with and without intralayer CNT/epoxy submicron filament reinforcement under flexural loading.

modulus of each composite. This can lead to a noticeable improvement of mechanical stability of the fabricated composites using these fibers as reinforcement layers, making them suitable for many applications such as aerospace and energy applications.

To check the quality of the fabricated submicron filament as a reinforcement for carbon fiber reinforced polymer (CFRP) prepreg composites. Thus, the layer of CNT/epoxy filaments has been deposited over a prepreg sheet and then stacked to make a panel. The final panel has eight layers of prepreg and seven layers of the CNT/epoxy filament sandwiched between layers. As a control, a panel with no CNT/epoxy filament has also been made. Short beam shear strength testing was conducted using the ASTM 2344D/M standard, load cell of 2.2 kN, a sample size of 2 mm \times 4 mm \times 12 mm, and a tolerance of 0.01 mm. Figure 9b reveals the load-displacement analysis of both CNT/epoxy and control panels. Here, the load values show that the integration on CNT/epoxy filaments improved the strength of the panels by up to 19 and 22% by adding reinforcement layer of 2 and 4 wt % CNT/epoxy filaments between prepreg layers. Furthermore, the fatigue test was also carried out with loading of a specimen at 60, 70, 80, 90, and 100 percentages of static failure loading for both panels. The test proved that the failure resistance has been improved by 100% after adding 4 wt % CNT/epoxy filaments as the reinforcement layer, while the presences of the aligned CNT improved the bonding between layers of prepreg.

CONCLUSIONS

Here, by electrospinning of a CNT/epoxy composite, submicron thermosetting filaments with embedded aligned CNT networks have been manufactured. Accordingly, the diameter of the fibers and thickness of the deposited layers could be precisely controlled using this method. Despite the fact that electrospinning a thermosetting polymer is still a challenge because of low viscosity of the solution and lack of plasticity, we were capable of making thermosetting polymers spinnable by developing a partial curing strategy through a thermal treatment process. Thus, spinnable viscosity and chemical bonding were properly achieved for electrospinning of the thermosetting polymer. Additionally, the very method helped to maintain the shape of the fiber; thus, multiple layers of the fibers were stacked uniformly without any interlayer deformation or diffusion. It was also observed that the addition of the CNT to the epoxy improved the mechanical modulus of the fibers by 49%, while reduced the porosity of the fabricated filaments by up to 25 percent. The addition of the CNT to the epoxy structure increased the mechanical properties of the polymer nanofibers, making them suitable for many composite applications. The obtained CNT/epoxy composites are promising for reinforcement of the structural composite parts and components in the aerospace, automotive, motorsports, and sporting goods because of their superior mechanical properties.

AUTHOR INFORMATION

Corresponding Authors

Hamid Dalir – Integrated Nanosystems Development Institute (INDI), Indiana University-Purdue University, Indianapolis, Indiana 46202, United States; Department of Mechanical and Energy Engineering, Indiana University-Purdue University, Indianapolis, Indiana 46202, United States; Multiscale Integrated Technology Solutions LLC,

Indianapolis, Indiana 46202, United States; Email: hdalir@iupui.edu

Mangilal Agarwal — Integrated Nanosystems Development Institute (INDI), Indiana University-Purdue University, Indianapolis, Indiana 46202, United States; Department of Mechanical and Energy Engineering, Indiana University-Purdue University, Indianapolis, Indiana 46202, United States; Multiscale Integrated Technology Solutions LLC, Indianapolis, Indiana 46202, United States; orcid.org/0000-0003-3039-0073; Email: agarwal@iupui.edu

Authors

Nojan Aliahmad – Integrated Nanosystems Development Institute (INDI), Indiana University-Purdue University, Indianapolis, Indiana 46202, United States

Pias Kumar Biswas — Integrated Nanosystems Development Institute (INDI), Indiana University-Purdue University, Indianapolis, Indiana 46202, United States; Department of Mechanical and Energy Engineering, Indiana University-Purdue University, Indianapolis, Indiana 46202, United States

Vidya Wable — Integrated Nanosystems Development Institute (INDI), Indiana University-Purdue University, Indianapolis, Indiana 46202, United States; Department of Mechanical and Energy Engineering, Indiana University-Purdue University, Indianapolis, Indiana 46202, United States

Iran Hernandez – Integrated Nanosystems Development Institute (INDI), Indiana University-Purdue University, Indianapolis, Indiana 46202, United States

Amanda Siegel – Integrated Nanosystems Development Institute (INDI), Indiana University-Purdue University, Indianapolis, Indiana 46202, United States; Multiscale Integrated Technology Solutions LLC, Indianapolis, Indiana 46202, United States

Complete contact information is available at: https://pubs.acs.org/10.1021/acsapm.0c00519

Notes

The authors declare no competing financial interest.

ACKNOWLEDGMENTS

The authors would like to express their gratitude to the National Science Foundation Small Business Technology Transfer (STTR) (#2036490) and the National Science Foundation Major Research Instrumentation Program by supporting this research (#1229514) for FESEM. Any opinions, findings, and conclusions or recommendations expressed in this material are those of the author(s) and do not necessarily reflect the views of the National Science Foundation. The authors would also like to thank Dr. Daniel Minner for his assistance with the instrumentation and proofreading, Reza Moheimani for BTU analysis, and Caroline Miller for TEM images.

REFERENCES

(1) Wang, Y.; He, J.; Chen, H.; Chen, J.; Zhu, R.; Ma, P.; Towers, A.; Lin, Y.; Gesquiere, A. J.; Wu, S.-T.; Dong, Y. Ultrastable, Highly Luminescent Organic-Inorganic Perovskite-Polymer Composite Films. *Adv. Mater.* **2016**, *28*, 10710–10717.

(2) Ling, T.; Wang, J.-J.; Zhang, H.; Song, S.-T.; Zhou, Y.-Z.; Zhao, J.; Du, X.-W. Freestanding ultrathin metallic nanosheets: Materials, synthesis, and applications. *Adv. Mater.* **2015**, *27*, 5396–5402.

- (3) Zhao, R.; Lu, X.; Wang, C. Electrospinning based all-nano composite materials: recent achievements and perspectives. *Compos. Commun.* **2018**, *10*, 140–150.
- (4) Gajanan, K.; Tijare, S. N. Applications of nanomaterials. *Mater. Today: Proc.* **2018**, *5*, 1093–1096.
- (5) Vijay Kumar, V.; Ramakrishna, S.; Kong Yoong, J. L.; Esmaeely Neisiany, R.; Surendran, S.; Balaganesan, G. Electrospun nanofiber interleaving in fiber reinforced composites-Recent trends. *Mater. Des. Process. Commun.* **2019**, *1*, No. e24.
- (6) Demir, M. M.; Horzum, N.; Taşdemirci, A.; Turan, K.; Güden, M. Mechanical Interlocking between Porous Electrospun Polystyrene Fibers and an Epoxy Matrix. ACS Appl. Mater. Interfaces 2014, 6, 21901–21905.
- (7) Reneker, D. H.; Yarin, A. L. Electrospinning jets and polymer nanofibers. *Polymer* **2008**, *49*, 2387–2425.
- (8) Wan, Y.-Q.; Guo, Q.; Pan, N. Thermo-electro-hydrodynamic model for electrospinning process. *Int. J. Nonlinear Sci. Numer. Simul.* **2004**, *5*, 5–8.
- (9) Theron, S. A.; Zussman, E.; Yarin, A. L. Experimental investigation of the governing parameters in the electrospinning of polymer solutions. *Polymer* **2004**, *45*, 2017–2030.
- (10) Aliheidari, N.; Aliahmad, N.; Agarwal, M.; Dalir, H. Electrospun Nanofibers for Label-Free Sensor Applications. *Sensors* **2019**, *19*, 3587
- (11) Mitchell, G. R. Electrospinning: Principles, Practice and Possibilities; Royal Society of Chemistry, 2015.
- (12) Teo, W. E.; Ramakrishna, S. A review on electrospinning design and nanofibre assemblies. *Nanotechnology* **2006**, *17*, R89.
- (13) Bhardwaj, N.; Kundu, S. C. Electrospinning: a fascinating fiber fabrication technique. *Biotechnol. Adv.* **2010**, 28, 325–347.
- (14) Huang, Z.-M.; Zhang, Y.-Z.; Kotaki, M.; Ramakrishna, S. A review on polymer nanofibers by electrospinning and their applications in nanocomposites. *Compos. Sci. Technol.* **2003**, *63*, 2223–2253.
- (15) Megahed, A. A.; Zoalfakar, S. H.; Hassan, A. E. A.; Ali, A. A. A novel polystyrene/epoxy ultra-fine hybrid fabric by electrospinning. *Polym. Adv. Technol.* **2018**, *29*, 517–527.
- (16) Zhang, F.; Zhang, Z.; Liu, Y.; Cheng, W.; Huang, Y.; Leng, J. Thermosetting epoxy reinforced shape memory composite microfiber membranes: Fabrication, structure and properties. *Composites, Part A* **2015**, *76*, 54–61.
- (17) Yao, Y.; Wang, J.; Lu, H.; Xu, B.; Fu, Y.; Liu, Y.; Leng, J. Thermosetting epoxy resin/thermoplastic system with combined shape memory and self-healing properties. *Smart Mater. Struct.* **2015**, 25, 015021
- (18) Neisiany, R. E.; Lee, J. K. Y.; Khorasani, S. N.; Ramakrishna, S. Self-healing and interfacially toughened carbon fibre-epoxy composites based on electrospun core-shell nanofibres. *J. Appl. Polym. Sci.* **2017**, *134*, 44956.
- (19) Guo, Y.; Yang, X.; Ruan, K.; Kong, J.; Dong, M.; Zhang, J.; Gu, J.; Guo, Z. Reduced graphene oxide heterostructured silver nanoparticles significantly enhanced thermal conductivities in hot-pressed electrospun polyimide nanocomposites. *ACS Appl. Mater. Interfaces* **2019**, *11*, 25465.
- (20) Wang, Y.; Yang, C.; Pei, Q.-X.; Zhang, Y. Some aspects of thermal transport across the interface between graphene and epoxy in nanocomposites. ACS Appl. Mater. Interfaces 2016, 8, 8272–8279.
- (21) Beckermann, G. W. Nanofiber interleaving veils for improving the performance of composite laminates. *Reinf. Plast.* **2017**, *61*, 289–293.
- (22) Johnsen, B. B.; Kinloch, A. J.; Mohammed, R. D.; Taylor, A. C.; Sprenger, S. Toughening mechanisms of nanoparticle-modified epoxy polymers. *Polymer* **2007**, *48*, 530–541.
- (23) Rosso, P.; Ye, L.; Friedrich, K.; Sprenger, S. A toughened epoxy resin by silica nanoparticle reinforcement. *J. Appl. Polym. Sci.* **2006**, 100, 1849–1855
- (24) Wang, Q.; Wu, W.; Gong, Z.; Li, W. Flexural progressive failure of carbon/glass interlayer and intralayer hybrid composites. *Materials* **2018**, *11*, 619.

- (25) Kuwata, M.; Hogg, P. J. Interlaminar toughness of interleaved CFRP using non-woven veils: Part 1. Mode-I testing. *Composites, Part A* **2011**, 42, 1551–1559.
- (26) Fiedler, B.; Gojny, F. H.; Wichmann, M. H. G.; Nolte, M. C. M.; Schulte, K. Fundamental aspects of nano-reinforced composites. *Compos. Sci. Technol.* **2006**, *66*, 3115–3125.
- (27) Xie, X.; Mai, Y.; Zhou, X. Dispersion and alignment of carbon nanotubes in polymer matrix: a review. *Mater. Sci. Eng., R* **2005**, *49*, 89–112.
- (28) Gojny, F.; Wichmann, M.; Fiedler, B.; Schulte, K. Influence of different carbon nanotubes on the mechanical properties of epoxy matrix composites A comparative study. *Compos. Sci. Technol.* **2005**, 65, 2300–2313.
- (29) Shaffer, M.; Sandler, J. Carbon nanotube/nanofibre polymer composites. In *Processing and Properties of Nanocomposites*; Advani, S. G., Ed.; World Scientific: New York, 2006; pp 1–60.
- (30) De Volder, M. F. L.; Tawfick, S. H.; Baughman, R. H.; Hart, A. J. Carbon nanotubes: present and future commercial applications. *science* **2013**, 339, 535–539.
- (31) Hussain, F.; Hojjati, M.; Okamoto, M.; Gorga, R. E. Review article: Polymer-matrix Nanocomposites, Processing, Manufacturing, and Application: An Overview. *J. Compos. Mater.* **2006**, *40*, 1511–1575.
- (32) Aitken, R. J.; Chaudhry, M. Q.; Boxall, A. B. A.; Hull, M. Manufacture and use of nanomaterials: current status in the UK and global trends. *Occup. Med.* **2006**, *56*, 300–306.
- (33) Ma, P.-C.; Siddiqui, N. A.; Marom, G.; Kim, J.-K. Dispersion and functionalization of carbon nanotubes for polymer-based nanocomposites: a review. *Composites, Part A* **2010**, *41*, 1345–1367.
- (34) Song, Y. S.; Youn, J. R. Influence of dispersion states of carbon nanotubes on physical properties of epoxy nanocomposites. *Carbon* **2005**, *43*, 1378–1385.
- (35) Giovannelli, A.; Di Maio, D.; Scarpa, F. Industrial-graded epoxy nanocomposites with mechanically dispersed multi-walled carbon nanotubes: static and damping properties. *Materials* **2017**, *10*, 1222.
- (36) Özden-Yenigün, E.; Menceloğlu, Y. Z.; Papila, M. J. MWCNTs/P (St-co-GMA) composite nanofibers of engineered interface chemistry for epoxy matrix nanocomposites. ACS Appl. Mater. Interfaces 2012, 4, 777–784.
- (37) Barra, G.; Guadagno, L.; Vertuccio, L.; Simonet, B.; Santos, B.; Zarrelli, M.; Arena, M.; Viscardi, M. Different Methods of Dispersing Carbon Nanotubes in Epoxy Resin and Initial Evaluation of the Obtained Nanocomposite as a Matrix of Carbon Fiber Reinforced Laminate in Terms of Vibroacoustic Performance and Flammability. *Materials* **2019**, *12*, 2998.
- (38) Roy, S.; Petrova, R. S.; Mitra, S. Effect of carbon nanotube (CNT) functionalization in Epoxy-CNT composites. *Nanotechnol. Rev.* **2018**, *7*, 475–485.
- (39) Singh, P. K.; Sharma, K.; Kumar, A.; Shukla, M. Effects of functionalization on the mechanical properties of multiwalled carbon nanotubes: A molecular dynamics approach. *J. Compos. Mater.* **2017**, *51*, *671*–*680*.
- (40) Ko, F.; Gogotsi, Y.; Ali, A.; Naguib, N.; Ye, H.; Yang, G. L.; Li, C.; Willis, P. Electrospinning of Continuous Carbon Nanotube-Filled Nanofiber Yarns. *Adv. Mater.* **2003**, *15*, 1161–1165.
- (41) Sen, R.; Zhao, B.; Perea, D.; Itkis, M. E.; Hu, H.; Love, J.; Bekyarova, E.; Haddon, R. C. Preparation of single-walled carbon nanotube reinforced polystyrene and polyurethane nanofibers and membranes by electrospinning. *Nano Lett.* **2004**, *4*, 459–464.
- (42) Kausar, A. Polyamide-grafted-multi-walled carbon nanotube electrospun nanofibers/epoxy composites. *Fibers Polym.* **2014**, *15*, 2564–2571.
- (43) Huang, Z.-M.; Zhang, Y.-Z.; Kotaki, M.; Ramakrishna, S. A review on polymer nanofibers by electrospinning and their applications in nanocomposites. *Compos. Sci. Technol.* **2003**, *63*, 2223–2253.
- (44) Bhardwaj, N.; Kundu, S. C. Electrospinning: a fascinating fiber fabrication technique. *Biotechnol. Adv.* **2010**, 28, 325–347.

- (45) Thompson, C. J.; Chase, G. G.; Yarin, A. L.; Reneker, D. H. Effects of parameters on nanofiber diameter determined from electrospinning model. *Polymer* **2007**, *48*, 6913–6922.
- (46) Ali, A. A.; Eltabey, M. M.; Farouk, W. M.; Zoalfakar, S. H. Electrospun precursor carbon nanofibers optimization by using response surface methodology. *J. Electrost.* **2014**, *72*, 462–469.
- (47) Matabola, K. P.; Moutloali, R. M. The influence of electrospinning parameters on the morphology and diameter of poly(vinyledene fluoride) nanofibers- effect of sodium chloride. *J. Mater. Sci.* **2013**, *48*, 5475–5482.
- (48) Zhang, C.; Yuan, X.; Wu, L.; Han, Y.; Sheng, J. Study on morphology of electrospun poly(vinyl alcohol) mats. *Eur. Polym. J.* **2005**, *41*, 423–432.
- (49) Haider, S.; Al-Zeghayer, Y.; Ahmed Ali, F. A.; Haider, A.; Mahmood, A.; Al-Masry, W. A.; Imran, M.; Aijaz, M. O. Highly aligned narrow diameter chitosan electrospun nanofibers. *J. Polym. Res.* **2013**, *20*, 105.
- (50) Kettle, J.; Ding, Z.; Horie, M.; Smith, G. C. XPS analysis of the chemical degradation of PTB7 polymers for organic photovoltaics. *Org. Electron.* **2016**, *39*, 222–228.
- (51) Williams, T.; Yu, H.; Woo, R.; Grigoriev, M.; Cheng, D.; Hicks, R. Atmospheric Pressure Plasma as a Method for Improving Adhesive Bonding; SME, 2014; p 2631.
- (52) Daneshkhah, A.; Vij, S.; Siegel, A. P.; Agarwal, M. Polyetherimide/carbon Black Composite Sensors Demonstrate Selective Detection of Medium-Chain Aldehydes Including Nonanal. *Chem. Eng. J.* **2020**, 383, 123104.
- (53) Zaldivar, R. J.; Nokes, J.; Steckel, G. L.; Kim, H. I.; Morgan, B. A. The effect of atmospheric plasma treatment on the chemistry, morphology and resultant bonding behavior of a pan-based carbon fiber-reinforced epoxy composite. *J. Compos. Mater.* **2010**, *44*, 137–156.
- (54) Naebe, M.; Lin, T.; Feng, L.; Dai, L.; Abramson, A.; Prakash, V.; Wang, X. Conducting Polymer and Polymer/cnt Composite Nanofibers by Electrospinning; ACS Publications, 2009.
- (55) He, X.-X.; Zheng, J.; Yu, G.-F.; You, M.-H.; Yu, M.; Ning, X.; Long, Y.-Z. Near-field electrospinning: progress and applications. *J. Phys. Chem. C* **2017**, *121*, 8663–8678.
- (56) Riaz, S.; Park, S.-J. Thermal and Mechanical Interfacial Behaviors of Graphene Oxide-Reinforced Epoxy Composites Cured by Thermal Latent Catalyst. *Materials* **2019**, *12*, 1354.
- (57) Damian, C.-M.; Pandele, A.; Iovu, H. Ethylenediamine functionalization effect on the thermo-mechanical properties of epoxy nanocomposites reinforced with multiwall carbon nanotubes. *UPB Sci. Bull.* **2010**, 72, 163.
- (58) Dollimore, D.; Heal, G. R. An improved method for the calculation of pore size distribution from adsorption data. *J. Appl. Chem.* **1964**, *14*, 109–114.
- (59) Drake, L. C. Pore-size distribution in porous materials. *Ind. Eng. Chem.* **1949**, *41*, 780–785.